Relationship between adsorbed fibronectin and cell adhesion on a honeycomb-patterned film

Sadaaki Yamamoto [1,2,*], Masaru Tanaka [1,2], Hiroshi Sunami [1,2], Keiko Arai [3], Aiko Takayama [2], Shigeko Yamashita [2], Yuka Morita [1], Masatsugu Shimomura [2, 3, 4]

1.Creative Research Initiative "Sousei" (CRIS), Hokkaido University, N21W10 Kita-ku, Sapporo 001-0021, Japan, 2. Core Research for Evolutional Science and Technology(CREST), Japan Science and Technology Agency (JST), Honchou 4-1-8, Kawaguchi 332-0012, Japan, 3. Spatio-Temporal Function Materials Research Group, Frontier Research System[3], RIKEN Institute, 1-12 Hirosawa, Wako. Saitama 351-0198, Japan, 4.Nanotechnology Research Center, Research Institute for Electronic Science, Hokkaido University[4], N12W6 Kita-ku, Sapporo 060-0812, Japan.

*Corresponding author. Tel:+81-11-706-9255, Fax:+81-11-706-9291; Email: syama@cris.hokudai.ac.jp

Abstract

Substratum surface morphology plays a vital roles in cellular behavior. Here, we characterized adsorption of fibronectin (Fn) as a typical cell adhesion protein onto honeycomb-patterned films made of poly(ε-caprolactone) (PCL) by using atomic force microscopy (AFM) and confocal laser scanning microscopy (CLSM). In oder to determine how cells adhere to a honeycomb-patterned film, focal adhesion of cardiac myocytes (CMYs) and endothelial cells (ECs) on the films were studied by using fluorescence labeling of vinculin. Fn adsorbs around the pore edges to form ring-shapes structures. CMYs and ECs adhere onto the honeycomb-patterned films at focal contact points localized around pore edges distributed over the entire cellular surface. The focal contact points on the honeycomb-patterned films correspond well with the adsorption sites of Fn. We suggest that the cell response to honeycomb-patterned films is associated with the adsorption pattern of Fn on the film.

Key words: Atomic force microscopy, Scanning electron microscopy, Cell adhesion, Adsorption, Self-assembly, Surface topography, Fibronectin, Tissue engineering

Introduction

Tissue engineering aims to restore, maintain, or improve complex human tissue function by using synthetic and living components [1]. Cells and the development of cytokines and scaffolds (cell-culture substrates) are key issues in tissue engineering. Since the original report that cells react to surfaces [2] , cell response to material surfaces has been an intriguing topic in tissue engineering. Extensive research has documented that surface properties such as chemistry, charge, rigidity, and topography play vital roles in cellular behavior, such as adhesion, spreading, migration, proliferation, and differentiation. Recently, cell culture substrates with geometric micro-and nano-patterns have been fabricated by various methods and have been extensively used to investigate how cells respond to surface topography [3-24]. Although the effects of nano- and micro-patterned topography on cell responses have been well documented, the mechanisms behind these effects remain unresolved.

Fibronectin (Fn) is representative of a class of important cell adhesion proteins that are found in blood and associated with cell surfaces [25]. When adsorbed onto biomaterials, Fn undergoes a conformational change from a globular structure to extended structure, depending on surface properties such as surface charge, hydrophobicity, hydrophilicity, and plays a critical role in mediating cell responses. To determine the role of Fn in mediating cell responses, adsorption of Fn both in molecularly isolated and aggregated states has been extensively investigated on various kinds of substrates, such as silica [26], methylated silica [26], mica [26,28] titanium [27], poly(metylmetacrylate) [28], sulfonated polystyrene [29], and glass [30] by using AFM, scanning electron microscopy (SEM), and fluorescence resonance energy transfer. Although adsorption of Fn is thus well-documented, little is known about the effect of substratum surface nano-and micro-pattern roughness on such adsorption [31].

Studies using biochemical methods suggest that structural changes in cell adhesion proteins such as fibronectin during adsorption onto a substrate determined by topography affect the molecular binding sites of these proteins to a receptor in cells, and thus affect the biological performance of these proteins and, ultimately, their critical role in mediating cell behavior [32,33]. Therefore, the correlation between the structures of adsorbed protein molecules and the substratum surface properties has been extensively researched. A detailed clarification of the effect of surface topography on protein adsorption requires a separation of the topographical and chemical effects, and, thus, requires a nano-

and microfabrication method to form geometrical patterns with no variation in surface chemical properties. We have previously reported that honeycomb-patterned porous polymer films can be prepared by simple casting of polymer solutions of a water-immiscible solvent under high humidity (about 80% relative humidity at 21±1℃) [11-13,21,34-36]. The pore size of the films can be controlled over a wide range, from hundreds of nanometers to hundreds of microns. By mechanical stretching a honeycomb-patterned film made of a viscoelastic polymer, pores of various shapes, such as hexagonal, elongated hexagonal, rectangular, square-like, or triangle-like, can be formed in a controlled way [24]. Our recent studies on the culture of cells, such as endothelial cells (EC), cardiac myocytes (CMYs), neural projenitor cells, and hepatocytes, on honeycomb-patterned films revealed that cellular behavior such as migration, spreading, and morphology can be controlled by the size and shape of pores of the film [11,13,19,21,24]. These characteristics of honeycomb-patterned films make these films suitable candidates for cell-culture substrates used in studying the effect of substratum surface morphology on the adsorption of adhesive proteins and the role that morphology plays in cell behavior.

On honeycomb-patterned films, the conformational change in adhesion protein molecules such as fibronectin required for focal contact adhesion is supposedly the mechanism behind this control. In this study, the effect of surface morphology on the structure of adsorbed Fn was assessed by using atomic force microscopy (AFM) and confocal laser scanning microscopy (CLSM). Further, in order to determine how cells adhere to a honeycomb-patterned film, focal adhesion of cardiac myocytes (CMYs) and endothelial cells (ECs) on the films were studied by using fluorescence labeling of vinculin. The results showed that the structure of adsorbed Fn depends on the surface morphology of the films. Based on the structure of adsorbed Fn, the focal contact points of both types of cells on a honeycomb-patterned film are probably determined by the structure of Fn, leading to the characteristic biological response of a honeycomb-patterned film different from that of a flat film.

Experimental Section

Materials

PCL and an amphiphilic copolymer (hereafter called Cap,) of dodecylamide and ω-carboxyhexylacrylamide were used in the film fabrication. PCL (Wako) has a molecular weight of 70,000-100,000. Cap was synthesized by a method previously reported [37]. Fn was a bovine plasma fibronectin (lyophilized from 0.05M

tris-buffer saline, pH7.5) purchased from Sigma. Water was purified using a Millipore system (Milli-Q, Millipore). Benzene, chloroform, and 10% formalin solution (Wako) were used without further purification.

Film Preparation

Honeycomb-patterned porous films (hereafter called honeycomb films) were fabricated on cover glasses (φ=15mm, Matsunami Glass Industry, Japan) by a method previously reported [24,34-36].

Adsorbed Fn assay

The quantity of adsorbed Fn onto the films was determined for different coating concentrations using bicinconic acid (BCA) as protein assay reagent (Pierce, IL) [29]. Different concentrations of Fn (0-1000 μg/ml) were adsorbed in 24-well tissue culture plates (Iwaki, Japan) for 24 h at 37 ℃ in 5% CO_2. The Fn solutions were removed from the plates, and then the films were washed two times in PBS. The reaction started at 37 ℃ after working reagent at 200 μl/well was added. After incubation for 2 h, 160 μl of the Fn solution was transferred into a 96-well plate for reading by a microplate reader (BiotrakII, Biochrom Ltd., U.K.) at the 590-nm wavelength.

AFM, CLSM, and SEM measurements

Tapping-mode AFM imaging was performed under ambient conditions using a Digital Instrument Nanoscope Ⅲa Multimode system (Digital Instrument, Santa Barbara CA) equipped with silicon nitride tips. The tips had a resonance frequency of ～300 kHz and a force constant of 14 N/m. The scan rate was 0.1-0.2 Hz, and the proportional and integral gains were set in the range of 2-10. CLSM measurements were performed using a CLSM apparatus (FLUOVIEW FV300, Olympus). The SEM images were obtained using a Hitachi S-3500N SEM (Hitachi, Japan) at an acceleration voltage of 15 kV. A 200-μl aliquot of 240 μg/ml bovine plasma Fn (Sigma, Munich Germany) in phosphate-buffered saline (PBS) was added to each honeycomb film and then incubated at 37 ℃ in 5% CO_2. The Fn-coated films were then gently washed with PBS, fixed with 10% formaldehyde (Wako) for 10 min at room temperature, permeabilized in PBS containing 1% normal goat serum and 0.1 % Triton X-100 for 30 min., and then the film was incubated for 1 h with anti-Fn antibody (diluted 1:500; Sigma). After being rinsed with water, the films were treated with fluoresein isothiocyanate (FITC)-conjugated anti-rabbit IgG antibody (diluted 1:2000). The specimens for SEM were sputter-coated with Au-Pd using a sputter-coating unit (Hitachi E1030, Hitachi, Japan).

Cell Culturing

CMYs were isolated by enzyme treatment of minced heart tissues of 19-day rat embryos (Sprague Dawley rats, Japan SLC, Inc) [38]. CMYs were seeded onto the pre-fabricated cell-culture substrates (i.e., a flat film and a self-supported honeycomb film) at a density of 1.0×10^5 cells/cm^2. Culture medium pre-warmed at 37 ℃ (Hepes-buffered Hams F10 containing 0.5% ITS and 3% FCS) was replaced daily. One day and three days after seeding, vinculin of CMYs was stained as follows. Cells were fixed by immersion in 4% paraformaldehyde (SIGMA) solution for 10min and permeabilized by immersion in 0.1% Triton X-100 (SIGMA) solution for 10 min. Cells were incubated for 1.5 h with mouse monoclonal anti vinculin IgG_1 antibodies (CHEMICON international, Inc) in 10% blocking solution (Dainippon Sumitomo Pharma) at 37 ℃. After washing with PBS, vinculin complex were visualized by incubation with Alexa Fluor 488 anti-mouse IgG antibodies (Molecular Probe) for 1 h at 37 ℃.

Porcine aortic endothelial cells (ECs, CSC Certificate ™ DAINIPPON PHARMACEUTICAL CO. LTD) were purchased. After the frozen cells were thawed at 45℃, they were resuspended into a culture medium (Duibecco's Modified Eagle's Medium, SIGMA) containing 10% FBS, 100 unit/ml penicillin, and 100 μg/ml streptomycin. A honeycomb film and a flat film on glass plates were preincubated in the culture medium for 72 h at 37 ℃ in 5% CO_2 before cell seeding. ECs (passage number of 6-8) were seeded on the films at a density of 1.5×10^4 cells/cm^2. Culture medium was replaced after days 1, 3, 5, and 7. To visualize the focal adhesion, vinculin was stained by using an immunological method with primary antibodies (diluted 1:100, CHEMICON) and fluorescence-labeled secondary antibodies (diluted 1;1000, Alexa Fluor 546 goat anti-mouse IgG, Molecular Probes). For immunostaining, cells were fixed by immersion in 10% formalin (Wako) at 20 ℃ for 10 min and permeated with 1% PBS solution of Triton X-100 for 5 min at 20 ℃.

Results and Discussion

Figure 1 shows SEM images of the structure of the PCL honeycomb film. The top-view image (Fig.1a) reveals a well-arranged hexagonal lattice. The side-view image (Fig.1c) reveals that the honeycomb films were porous with a double-layered structure in which two hexagonal lattices were connected vertically by pillars at the vertex of hexagons. A schematic model of this double-layered structure is shown in Fig. 1d.

The amount of Fn adsorbed on both the flat and honeycomb films was measured as a function of incubation time and of Fn-coating concentration

determined by using a total adsorbed protein assay. The amount of Fn adsorbed on both films increased linearly with incubation time up to 1 h, and then became saturated . With increasing Fn-coating concentration up to 50 μg/ml, Fn adsorption on the flat film increased drastically and then saturated when the Fn-coating concentration reached 600 μg/ml. Although the adsorption behavior on the honeycomb films was similar to that on the flat films, the amount of Fn adsorbed on the honeycomb films was twice that on the same size of flat films. Considering the three-dimensional porous structure of the honeycomb films (Fig.1), the higher amount of adsorbed Fn might be due to the larger surface area of the film. This possibility is supported by the depth profile of the fluorescence intensity from stained Fn obtained by scanning excitation laser light from top to bottom of the films in CLSM. In the depth profile, fluorescence was observed only at the top and bottom surfaces of the honeycomb films and not within the film (data not shown), suggesting that Fn adsorbed onto the top (front and rear sides of the top layer) and bottom layer of a honeycomb film. Because the ratio of pore area to total surface area (porosity) of a top sheet is about 0.5, the estimated surface area of a honeycomb film for Fn adsorption is about twice that of a flat film, and thus the amount of Fn adsorbed on a honeycomb film should be about twice that on a flat film. The amount of adsorbed Fn at saturation on a flat film was 0.52 μg and that on a honeycomb film was 0.91 μg. The surface density at saturation on a flat film calculated using the surface area of a flat film (1.32 cm^2) and the adsorbed amount (0.52 μg) was about 0.4 μg/cm^2. This value agrees well with the approximate amount of Fn required for monolayer coverage, namely, 0.32 μg /cm^2 , based on reported estimates of the dimension of a Fn molecule [32,33,39,40]. Based on the estimated surface area of a honeycomb film (twice the surface area of a flat film), the surface density of Fn on a honeycomb film is equal to that on a flat film. The total adsorbed protein assay revealed a monolayer-level adsorption behavior of Fn on both the flat and honeycomb films.

Figure 2a shows AFM images of the surface of a flat film at 48 h incubation in 240 μg/ml Fn/PBS solution at 25 ℃. Despite the monolayer-level adsorption, the surface was not uniform but had an interconnected fibrillar structure. Typical fibrils reached 30-50 μm in length, 0.5-2 μm in width, and 0.05-0.2 μm in height (AFM image shown in Fig. 2b). The CLSM image of stained Fn adsorbed on the flat films revealed a fibrillar structure similar to that revealed by AFM (Fig.2c). Both images indicate that Fn adsorbs on the flat films to form aggregates with a fibrillar structure, similar to that of Fn adsorbed onto sulfonated polystyrene films [29],

supporting our assignment that the fibril-like aggregates are adsorbed Fn.

Both CLSM and AFM images reveal that adsorption structure of Fn on a honeycomb film depend on incubation time up to 48 h (Fig. 3). Both images show that the surface of the honeycomb film after incubation in Fn/PBS solution completely differs from that of a flat film and depends on the incubation time. At an incubation time of 0 h, the surface is flat. At 24 h incubation, distinctly different morphologies coexist on the surface (AFM image in Fig. 3a); the surface above the dashed line in Fig.3a is covered by numerous globules, whereas the surface below the dashed line is uniform. The distribution of the fluorescence from stained Fn in the CSLM image corresponds well to the morphological differences observed in the AFM image (Fig. 3b). By 48 h incubation, a few globules remain, and ring structures about 100 nm high and 1 μm wide appear around the pores as a dominant structure. Several rings were scraped off while repeating the tip scanning (as shown by white arrows in Fig. 3c). The CLSM image (Fig. 3d) reveals strong ring-like fluorescence along the pore edges, corresponding well to the ring structures evident in the AFM images. AFM image (Fig. 3e) reveals that the surface of the honeycomb films incubated in PBS solution between 0 and 48 h without Fn is uniform, and shows no evidence of any adsorbates. Both AFM and CLSM images reveal that Fn adsorbed and underwent a structural transition from globular form on the rim of the film to ring form around the edges of pores. A similar time-dependent self-organization of Fn has been reported for adsorption of Fn onto a sulfonated polystyrene surface [29], although the amount of adsorbed Fn was much higher than that for the honeycomb films used in our study.

The amount of adsorbed Fn on both films remains relatively constant, regardless of incubation time (longer than 1 h). Furthermore, the morphologies of the aggregates depend on the substrate surface structure (note that the chemical composition of both the honeycomb films and flat films was the same). Because protein molecules bound to a surface can rearrange via conformational changes [41] and diffusion [42], three-dimensional aggregate formation is possible, even for molecules adsorbed irreversibly with random orientations without overlapping or closed-packed monolayer density [43]. The structural transition from globular form to fibrillar form can be ascribed to the self-organization of adsorbed Fn caused by the dependence of diffusion on the surface morphology (honeycomb pattern and flat surface). Protein organization on a patterned surface has been reported for Fn adsorption onto Au/Si micropatterns coated by a sulfonated polystyrene film [31]. Fn was adsorbed on the Si regions of the substrate but was repulsed by the Au

domains, resulting in a structure of self-assembling Fn determined by the width of Si domains. The possible mechanism behind this Fn organization on the patterned surface is the balance between the bending energy of Fn and the unfavorable energy of contact with the Au interface. In our current study, the width of a rim of a honeycomb film on which Fn adsorbed was about 5 μm. The width of a rim and the size of a pore are comparable to the width of Si and Au domains of Au/Si micropatterns (several microns to 20 microns). If pores play a role similar to the role that Au domains play, namely, that Fn does not adsorb, the same mechanism might be responsible for the self-organization of Fn on a honeycomb film.

To determine how cells adhere to a honeycomb film, vinculin within focal adhesions and actin cytoskeleton linked to integrin receptor in cell membranes were examined here by using immunofluorescence staining (Fig. 4). The focal contact points on a flat film clearly depend on the cells; EC adheres onto a flat film at cell peripheries and focal adhesions are very faint, whereas the focal contact points of CMYs are located randomly over entire cell bodies and the focal adhesions are strongly evident. Focal adhesion differs significantly between the honeycomb films and flat film. On the honeycomb films, focal adhesions of both types of cells are distributed over the entire cellular surface and located around the edges of pores lying beneath the cell bodies. Focal adhesion formation and subsequent actin polymerization are essential to a cell's ability to adhere. Integrin receptors recognize a specifically distinct peptide sequence of Fn (cell-binding RGD integrin recognition motif) that mediates cell-substrate focal contact adhesion. Binding of adhesion receptors to adsorbed Fn provides mechanical coupling to the underlying substrate and activates signal transductive pathways that control cellular behavior such as proliferation and differentiation [44]. The location of focal contact points corresponds well with the adsorption sites of Fn, suggesting that the focal adhesion pattern on honeycomb films is determined by the adsorption pattern of Fn. Focal contact points are regularly aligned on the honeycomb films. This adhesion pattern implies that the distance between adjacent focal contact points and/or the density of focal contact points are determined precisely by the pore size, and this distance and/or density might play a vital role in activating the signal transductive pathways. This control of focal contact points by the pore size might be an origin of the pore-size dependence of cell response characteristics to a honeycomb film.

Summary

In this study, the adsorption structure of Fn and the adhesion patterns of ECs and CMYs on honeycomb films and flat films was studied, and the role the honeycomb film plays on cell response were discussed. Results showed that the structure of adsorbed Fn was determined by the micro-pattern pores of the honeycomb film and by incubation time. The structure of adsorbed Fn changed with increasing incubation time from globular to fibril-like form. The fibril-like aggregates were located on the periphery of micro-pores. The focal contacts of the cells located on the periphery of the micro-pores are apparently determined by the fibril-like form of adsorbed Fn. We suggest that the cell response to the honeycomb-patterned film is associated with the ordered adsorption pattern of Fn on the honeycomb film, leading to the characteristic response of a honeycomb film different from that of a flat film. The results presented here suggest a mechanism where the structure of the adsorbed cell adhesion proteins determined by a substrate micro-pattern affects the molecular binding sites of the proteins to a receptor in cells, affects the biological performance of the proteins and, thus ultimately affects their critical role in mediating cell behavior.

Acknowledgements

This study was supported by a Special Coordination Funds for Promoting Science and Technology, Ministry of Education, Culture, Sports, Science and Technology, Japan (Mext), CREST-JST (Grants-in-Aid from the Japan Science and Technology Corporation)

References

[1] R. Langer and J. P. Vacanti, Science, 260 (1993) 920.

[2] A. Carrel and M. Burrows, J. Exp. Med. 13 (1911) 571.

[3] J. A. Hubbel, Bio/Technology 13 (1996) 565.

[4] C. S. Chen, M. Mrksich, S. Huang, G. M. Whitesides and D. E. Ingber, Science, 276 (1997) 1425.

[5] A. M. Green, J. A. Jansen, J-P. C. M. van der Waerden and A. F. von Recum, J. Biomed. Mater. Res. 28 (1994) 647.

[6] S. Turner, L. Kam, M. Isaacson, H. G. Graighead, W. Shain and J. Turner, J. Vac. Sci. Technol. 15 (1997) 2848.

[7] A. Curtis and C. Wilkinson, Biomaterials, 18 (1997) 1573.

[8] R. S. Kane, S. Takayama, E. Ostuni, D. E. Ingber and C. M. Whiteside, Biomaterials, 20 (1999) 2363.

[9] E. T. den Braber, J. E. de Reijter, L. A.Ginsel, A. F. van Recum and J. A. Jansen, J. Biomed. Mater. Res. 40 (1998) 291.

[10] A. Folch and M. Toner, Biotechnol. 14 (1998) 388.

[11] T. Nishikawa, J. Nishida, R. Ookura, S. Nishimura, S. Wada, T. Karino and M. Shimomura, Mater. Sci. Eng. C8-9 (1999) 495.

[12] T. Nishikawa, J. Nishida, R. Ookura, S. Nishimura, S. Wada, T. Karino and M. Shimomura, Mater. Sci. Eng. C10 (1999) 141

[13] K. Sato, K. Hasebe, M. Tanaka, M. Takebayashi, K. Nischikawa, M. Schimomura, T. Kawai, M. Matsushita and S. Todo, Int. J. Nanosci. 1 (2002) 689.

[14] H. G. Graighead, C. D. James and A. M. P. Turner, Curr. Opi. Sol. State Mater. Sci. 5 (2001) 177.

[15] A. Mata, C. Boehm, A. J. Fleischman, G. Muschlar and S. Roy, J. Biomed. Mater. Res. 62 (2002) 499.

[16] M. Arnold, A. E. Cavalcanti-Adam, R. Glass, J. Blümmel, W. Eck, M. Kantlehner, H. Kessler and J. P. Spatz, ChemPhysChem 5 (2004) 383.

[17] X. F. Walboomers, L. A. Ginsel and J. A. Jansen, J. Biomed. Mater. Res, 51 (2000) 529.

[18] N. M. Dowell-Mesfin, M-A. Abdul-Karim, A. M. P. Turner, S. Scanz, H. G. Craighesd, B. Roysam, J. N. Turner and W. Shain, J. Neural Eng. 1 (2004) 78

[19] A. Tsuruma, M. Tanaka, N. Fukushima and M. Shimomura, e-J. Surf. Sci. Nanotech. 3 (2005) 159.

[20] M. J. Dalby, M. O. Riehle, D. S. Sutherland, H. Agheli and A. S. G. Gurtis, J. Biomed. Mater. Res 69A (2004) 314.

[21] T. Nishikawa, J. Nishida, R. Ookura, H. Ookubo, H. Kamachi, M. Matsushita, S. Todo and M. Schimomura, Stud. Surf. Sci. Catl. 132 (2001) 132, 509.

[22] F. A. Denis, P. Hanarp, D. S. Sutherland, J. Gold, C. Mustin, P. G. Rouxhet and Y. F. Dufrêne, Langmuir 18 (2002) 819.

[23] M. J. Dalby, S. Childs, M. O. Riehle, H. J. H. Johnstone, S. Affrossman and A. S. G. Curtis, Biomaterials, 24 (2003) 927.

[24] T. Nishikawa, M. Nonomura, K. Arai, J. Hayashi, T. Sawadaishi, Y. Nishiura, M. Hara and M. Shimomura, Langmuir, 19 (2003) 6193.

[25] R. O. Hynes, Fibronectin, (New York, Springer 1990) p546.

[26] M. Bergkvist, J. Carlsson and S. Oscarsson, J. Biomed. Mater. Res. 64A (2003) 349.

[27] D. E. MacDonald, B. Markovic and M. Allen, J. Biomed. Mater. Res. 41 (1998) 120.

[28] E. R. Zenhausen, M. Jobin, M. Taborelli and P. Descounts, Ultramicroscopy, 42-44(Pt B) (1992) 1155.

[29] N. Pernodet, M. Rafailovich, J. Sokolov, D. Xu, N-L.Yamg and K. J. McLeod, Biomed. Mater. Res. 64A (2003) 684.

[30] L. Bough and V. Vogel, J. Biomed. Mater. Res. 69 (2004) 525.

[31] N. Pernodet, S. Lenny, J. John and R. Miriam, American Phys. Soc., March Meeting 2004, March 22-26, 2004,Palais des Congress de Montreal, Montreal, Quebec, Canada, Meeting ID; MAR04, abstract#P9.011

[32] A.G. Garcia, M. D. Vega and D. Boettinger, Mol. Biol. Cell, 10 (1999) 785.

[33] A. G. Garcia and D. Boettinger, Biomaterials, 20 (1999) 2427.

[34] N. Maruyama, T. Koito, J. Nishida, T. Sawadaishi, X. Gieren, K. Ijiro, O. Karthaus and M. Shimomura, Thin Solid Films, 854 (1998) 327.

[35] T. Nishikawa, R. Okura, J. Nishida, K. Arai, J. Hayashi, N. Kurono, T. Sawadaishi, M. Hara and M. Schimomura, Langmuir 18 (2002) 5734.

[36] M. Tanaka, M. Takebayashi, M. Miyama, J. Nishida and M. Schimomura, Bio-Med. Mater. Eng. 14 (2004) 439.

[37] S. Nishimura and K. Yamada, J. Am. Chem. Soc. 119 (1997) 10555.

[38] M. C. Denyer, M. Riehle, M. Scholl, C. Sproessler, S. T. Britland, A. Offenhaeusser and W. Knoll, In Vitro Cell. Dev. Biol. Anim. 35 (1999) 352.

[39] F. Grinnel and M. K. Feld, J. Biomed. Mater. Res. 15 (1981) 363.

[40] E. C. Williams, P. A. Janmey, J. D. Ferry and D. F. Mosher,; J. Biol. Chem. 257 (1982) 14973.

[41] W. G. Pitt, S. H. Spiegelberg and S. L. Cooer, in: Proteins at interfaces Physicochemical and Biochemical Studies (J. L. Brash and T. A. Horbett). ACS Symposium series, p.324. Amer. Chem. Soc. Washinton, DC,1987.

[42] R. D. Tilton, C. R. Robertson and A. P. Gast, J. Colloid Interface Sci.137 (1990) 192.
[43] P. A. Dimilla, S. M. Albelda and J. A. Quinn, J. Collid Interface Sci. 153 (1992) 212.
[44] K. Buridge and M. Charanowska-Wodnick, Ann. Rev. Cell Dev. Biol. 12 (1996) 463

Figure captions

Figure 1. SEM images of a honeycomb-patterned film. (a) top view, (b) tilted view, (c) side view, and (d) schematic of the double-layered structure of the film.

Figure 2. (a) Topographic AFM image , (b) cross-sectional profile along the dotted line in (a), and (c) CLSM image of Fn adsorbed on a flat film observed after 48 h incubation in 1 ml of 240 μg/ml Fn/PBS solution at 25 ℃

Figure 3. AFM and CLSM images showing the morphology of adsorbed Fn as a function of incubation time in a PBS solution of Fn. (a) AFM image at 0 hr incubation time. (b) AFM and (c) CLSM images at 20 h incubation time. Dashed line indicates the boundary separating two domains where morphology and fluorescence intensity differ. (d) AFM image at 48 h incubation time. (e) AFM image of surface after several scans on the surface of (d), where ring-like structures were scraped off by the scanning (compare areas indicated by white arrows in (d)). (f) Close-up image of area enclosed by dashed line in (d). (g) Cross-sectional profile along dotted line in (f). (h) CLSM image at incubation time of 48 h.

Figure 4. CLSM images of (a) endothelial cells (ECs) (shown in red) and cardiac myocytes (CMYs) (shown in green) immunofluorescence stained for vinculin (focal contacts) on honeycomb-patterned film and flat film after 72 h incubation. (a) and (c) on a honeycomb film, (b) and (d) on a flat film. Locations of focal contact points around the edges of pores are clearly evident.

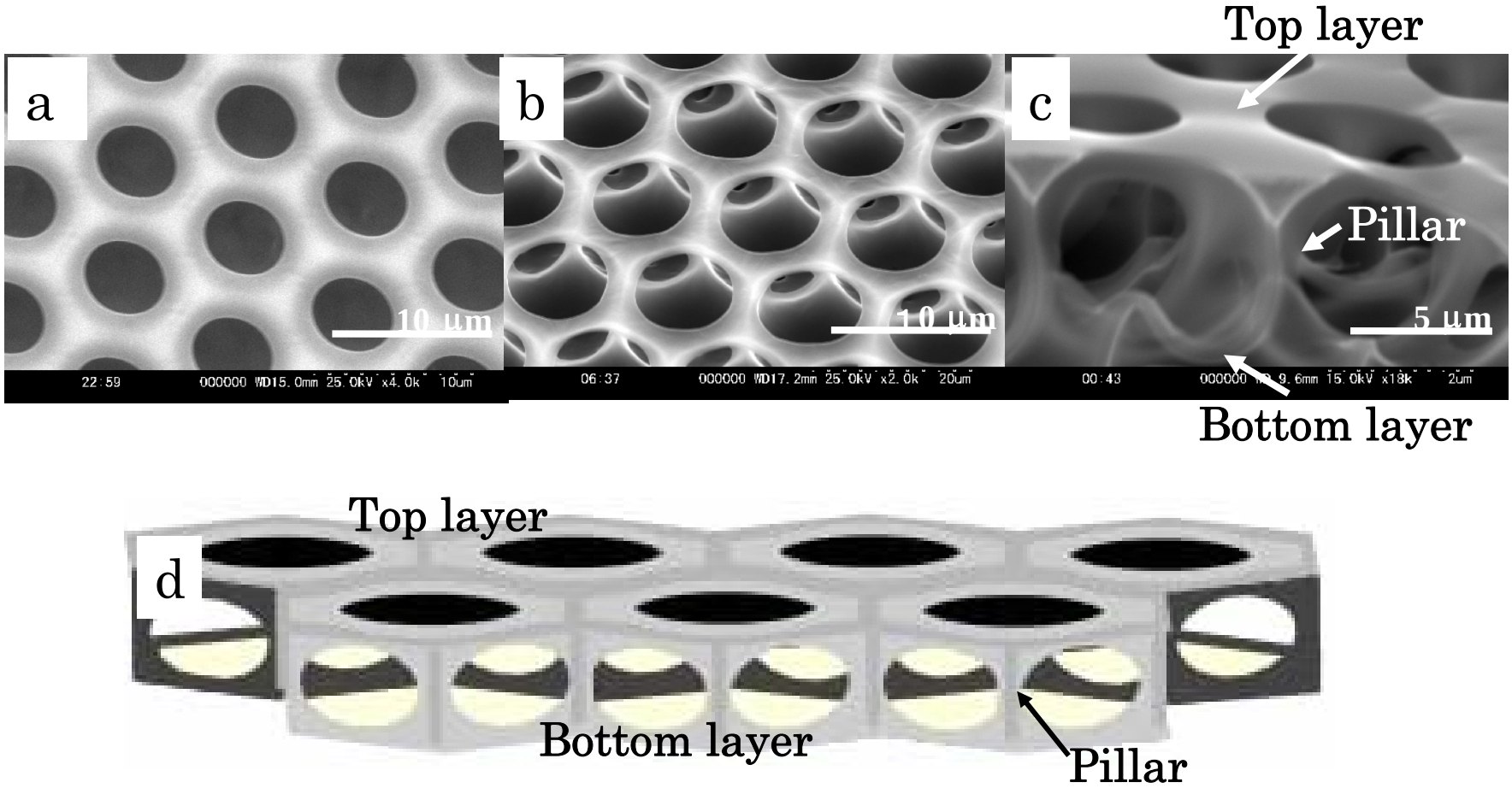
a
10 μm
b
10 μm
c
Top layer
Pillar
5 μm
Bottom layer
d
Top layer
Bottom layer
Pillar

Figure 1

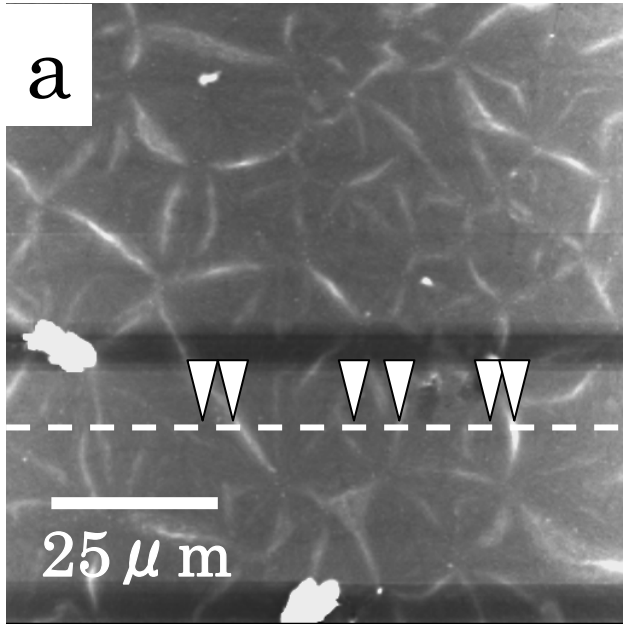
a
25 μ m

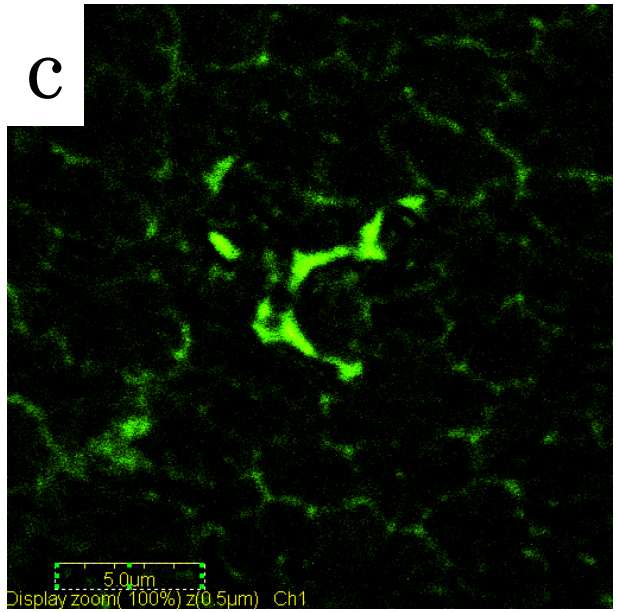
c
5.0μm
Display zoom(100%) z(0.5μm) Ch1

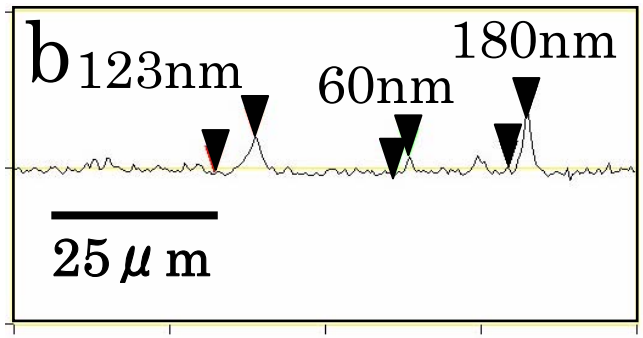
b
123nm
60nm
180nm
25 μ m

Figure 2

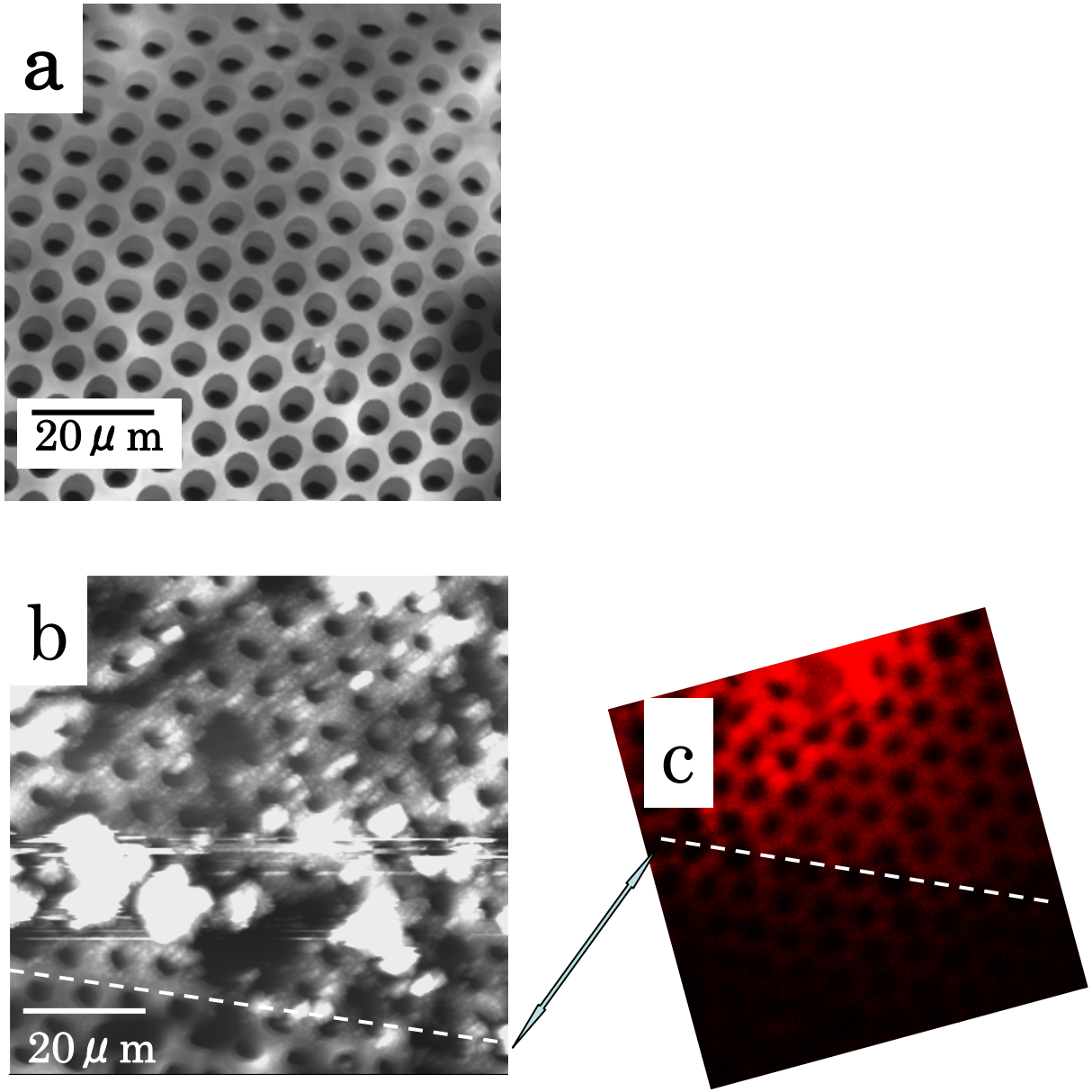

Figure 3

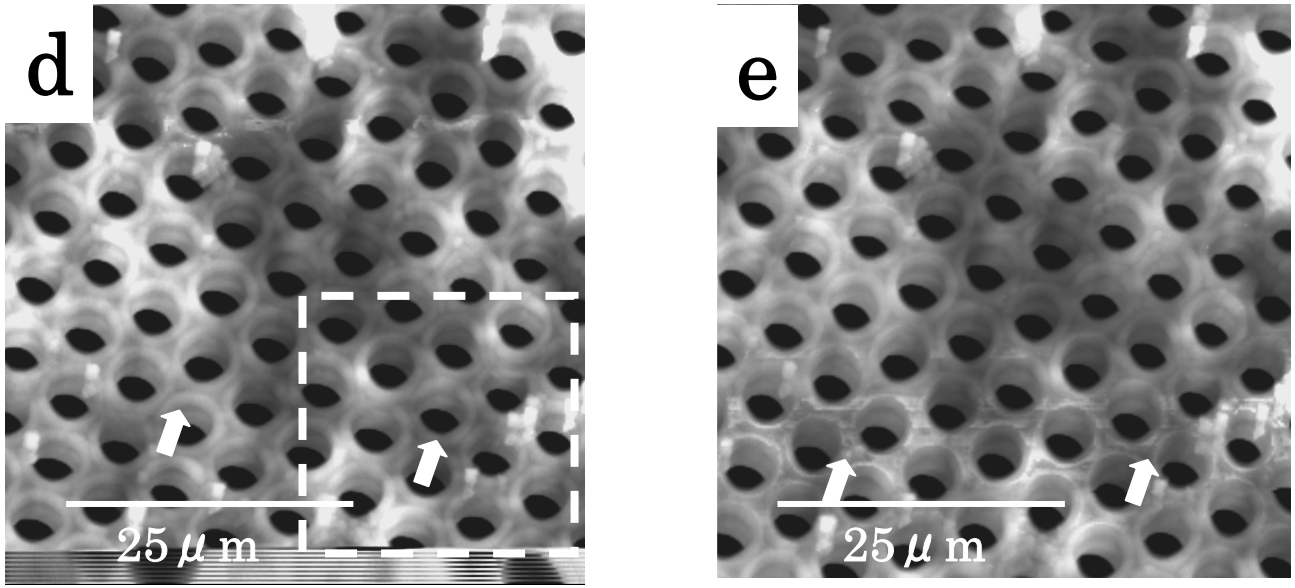

Figure 3

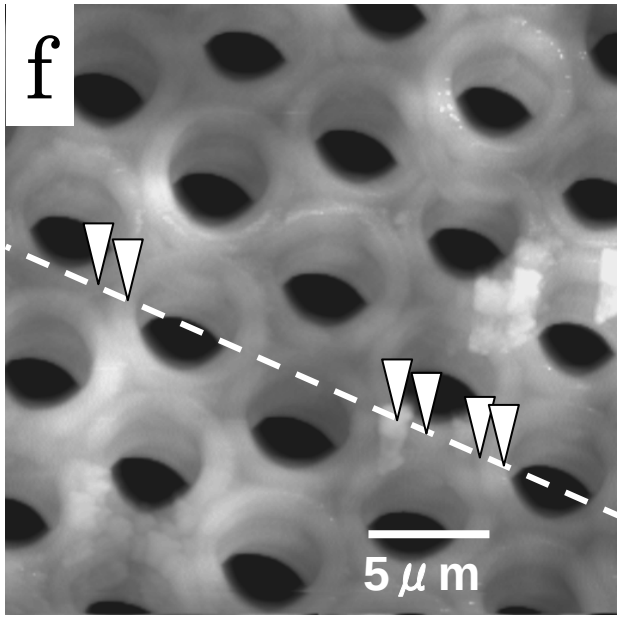

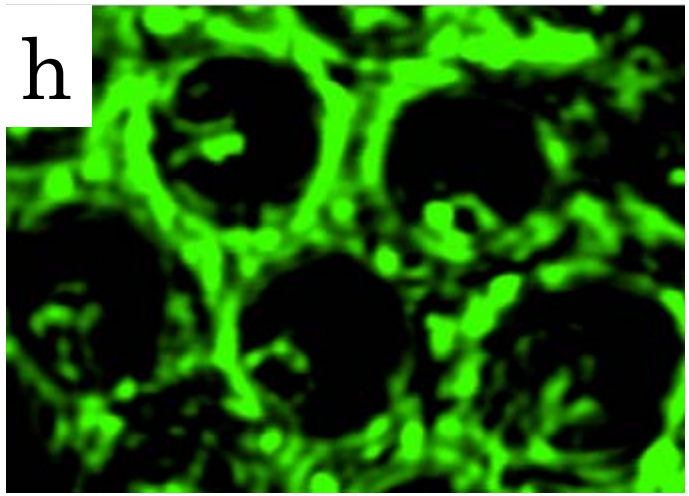

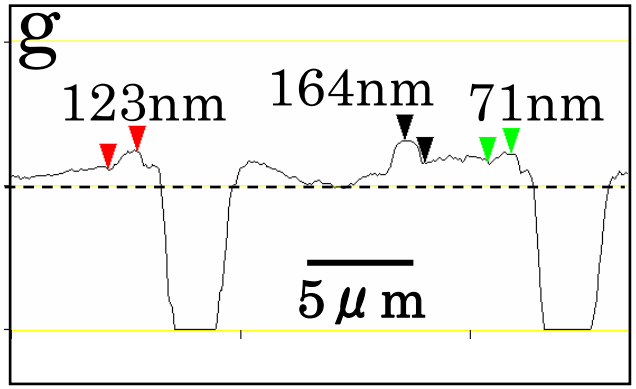

Figure 3

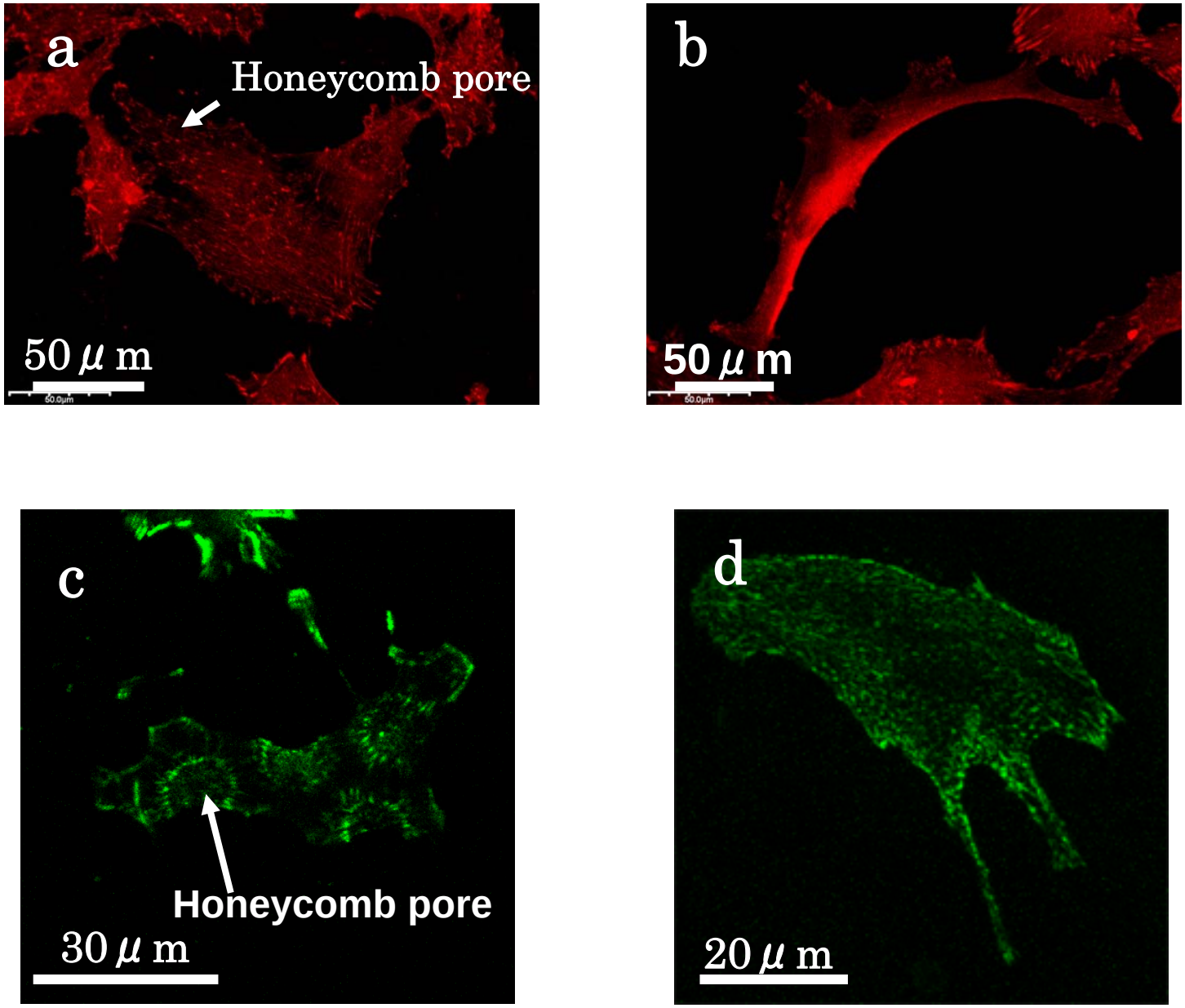

Figure 4